PNAS
www.pnas.org

Supplementary Information for

Siglecs-7/9 function as inhibitory immune checkpoints *in vivo* and can be targeted to enhance therapeutic antitumor immunity

Itziar Ibarlucea-Benitez, Polina Weitzenfeld, Patrick Smith, Jeffrey V. Ravetch*

Jeffrey V. Ravetch
Email: ravetch@rockefeller.edu

This PDF file includes:

Figures S1 to S5

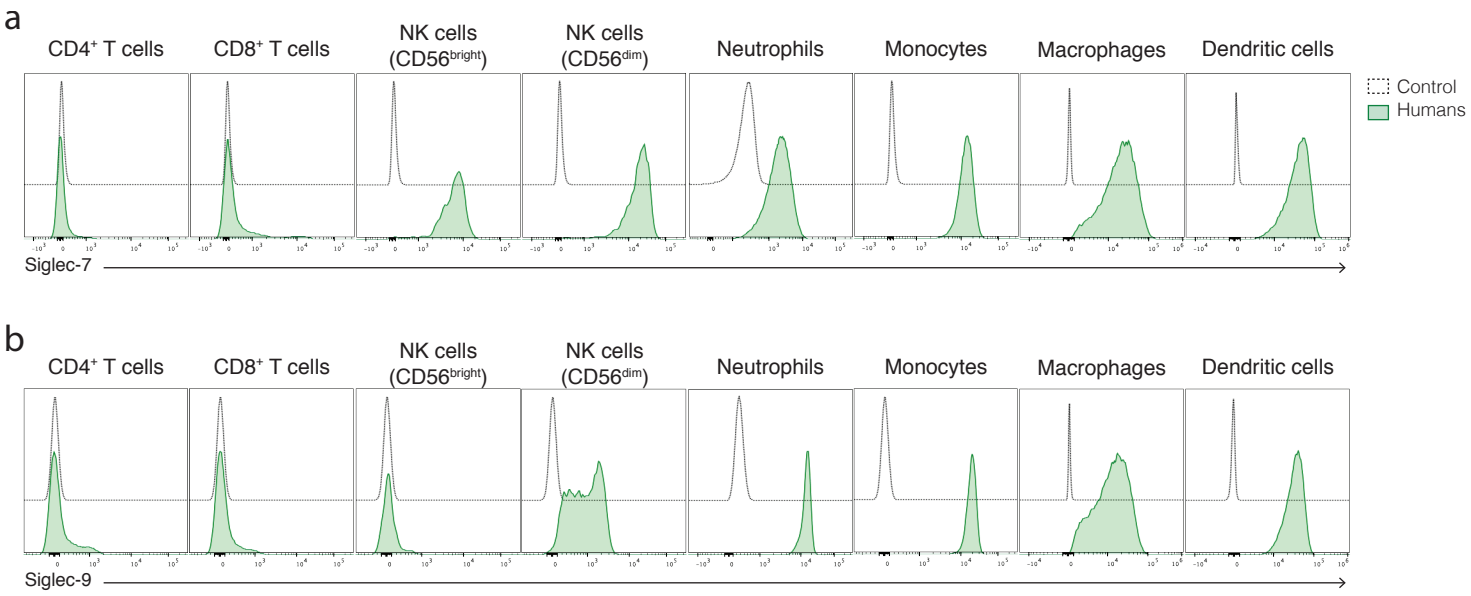

Figure S1: Expression of Siglec-7 and Siglec-9 on human PBMCs.
(a) Surface expression of Siglec-7 or **(b)** Siglec-9 on immune populations of human PBMCs (green) compared to an unstained control (dashed line). Panels show a representative donor from a representative experiment (n = 2 experiments).

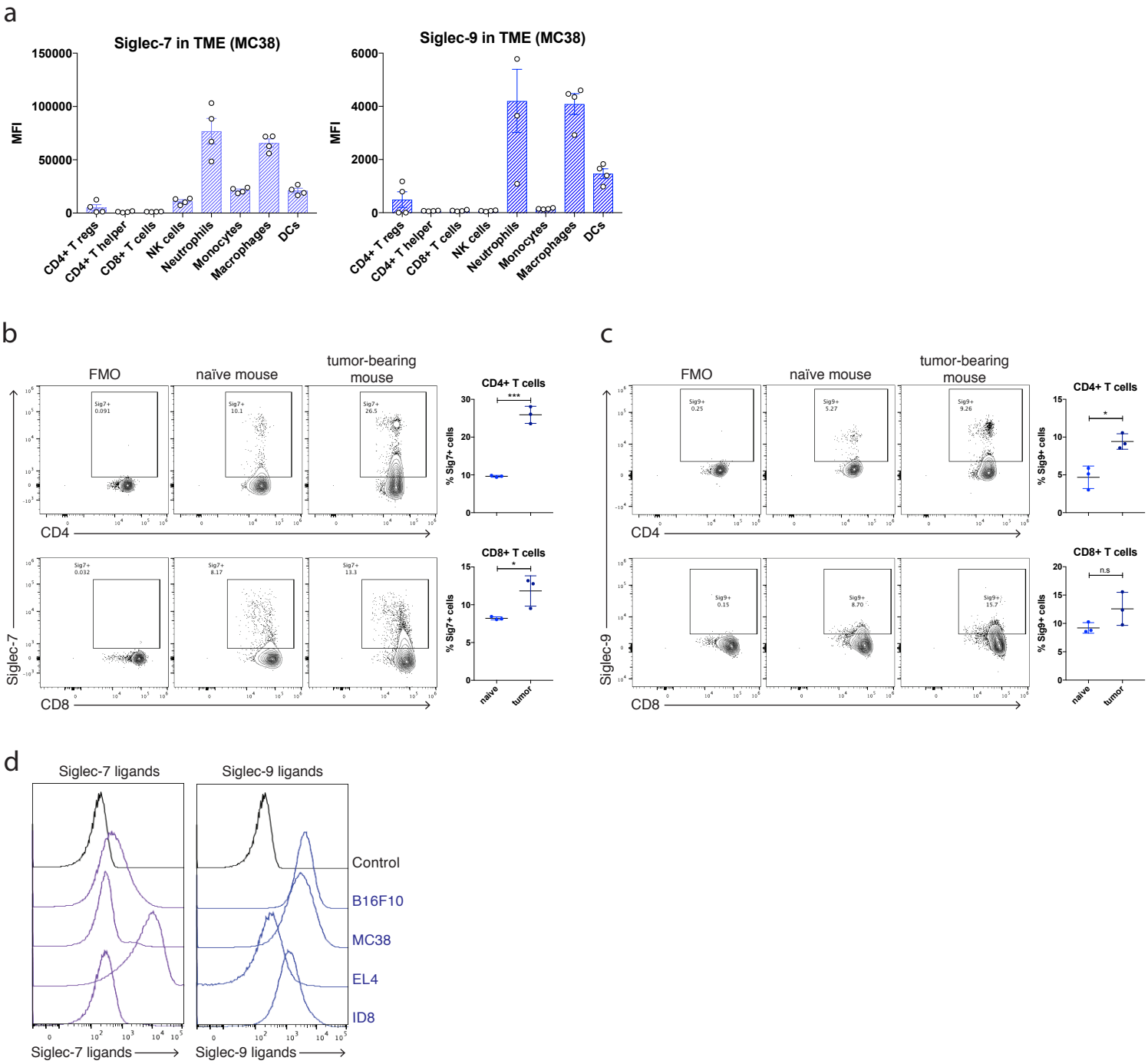

Figure S2: Characterization of Siglec-7/9 Siglec-E KO mice.

(a) Expression of Siglec-7 (left) or Siglec-9 (right) on infiltrated TILs in MC38 tumors in Siglec-7/9 Siglec-E KO mice, expressed as median fluorescence intensity (MFI), each circle represents one mouse. Data are displayed as mean ± SEM. Panels show a representative experiment (n = 2). **(b)** Expression of Siglec-7 on CD4+ T cells (top row), or on CD8+ T cells (bottom row) of naïve or tumor bearing Siglec-7/9 Siglec-E KO mice. Graphs show percentage of CD4+ T cells (top) or CD8+ T cells (bottom) that express Siglec-7. **(c)** Expression of Siglec-9 on CD4+ T cells (top row), or on CD8+ T cells (bottom row) of naïve or tumor bearing Siglec-7/9 Siglec-E KO mice. Graphs show percentage of CD4+ T cells (top) or CD8+ T cells (bottom) that express Siglec-9. n = 3 mice/group. *p < 0.05; ***p < 0.005; ns, non-significant (unpaired 2-tailed t test). **(d)** Surface expression of Siglec-7 ligands (left) or Siglec-9 ligands (right) on the indicated murine tumor cell lines. Cells were incubated with either a Siglec-7 or a Siglec-9 - Fc fusion (human IgG), followed by a PE-conjugated anti-human IgG secondary antibody. Panel shows a representative experiment (n=2).

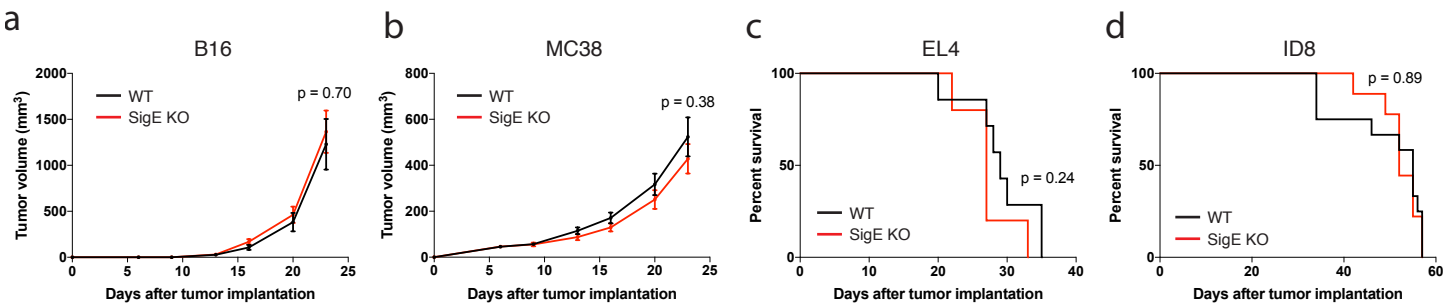

Figure S3: Impact of Siglec-E on progression of several mouse tumor models.
(a) Tumor growth or overall survival of WT C57BL/6 (black) and Siglec-E KO (red) mice inoculated with B16 melanoma (s.c.), **(b)** MC38 colon carcinoma (s.c.), **(c)** EL4 lymphoma (i.v.), and **(d)** ID8 ovarian carcinoma (i.p.). P values for each graph are indicated (B16 and MC38: unpaired 2-tailed t test; EL4 and ID8: log-rank test).

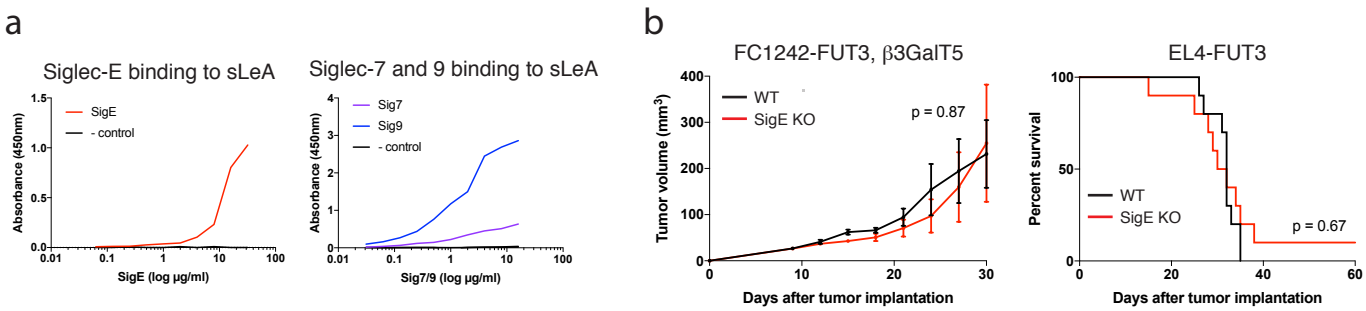

Figure S4: Sialyl-Lewis A is a ligand of Siglec-E, Siglec-7 and Siglec-9.
(a) An ELISA 96-well plate was coated with recombinant sLeA (CA19-9), unbound carbohydrate was washed, and wells were incubated with serial dilutions of Siglec-E – mFc (left, red), Siglec-7 – hFc (right, purple), or Siglec-9 – hFc (right, blue). CD19 – mFc or CTLA4 – hFc (black) were used as a negative control. Binding to sLeA was detected by an HRP-conjugated anti-mIgG or an HRP-conjugated anti-hIgG. **(b)** Tumor growth kinetics or overall survival curves of WT C57BL/6 (black) and Siglec-E KO (red) mice inoculated with a FC1242-FUT3, β3GalT5 pancreatic carcinoma cells (s.c., left), or EL4-FUT3 lymphoma cells (i.v., right). P values for each graph are indicated (FC1242-FUT3, β3GalT5: unpaired 2-tailed t test; EL4-FUT3: log-rank test). n = 6 or 10 mice/group, respectively.

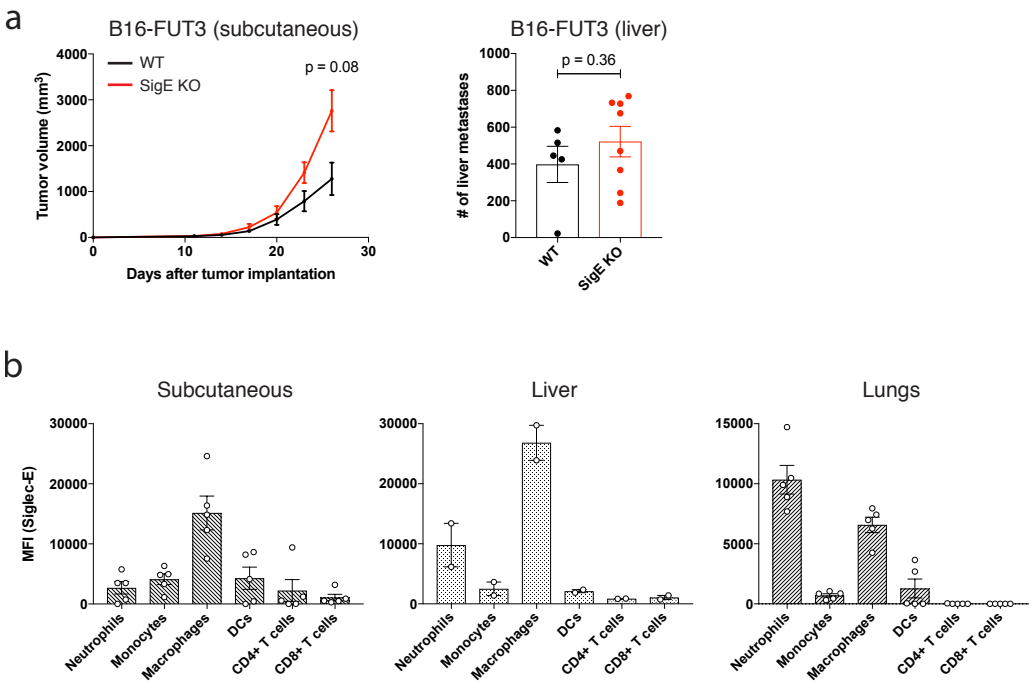

Figure S5: The tumor microenvironment dictates the role of Siglec-E in tumor progression.

(a) Tumor growth kinetics of WT C57BL/6 (black) and Siglec-E KO (red) mice bearing B16-FUT3 subutaneous tumors or B16-FUT3 liver tumors. P values for each graph are indicated (unpaired 2-tailed t test). **(b)** MFI of Siglec-E on immune populations infiltrating B16-FUT3 tumors located in different organs: left, subcutaneous; middle, liver; right, lung. Data are displayed as mean ± SEM, n = 2 mice/group.